Article

Quantitative analysis of desertification driving mechanisms in the Shiyang River Basin: Examining interactive effects of key factors through the Geographic Detector Model

Maurice Ngabire[1,2], Tao Wang[1,2], Jie Liao*[1,2], Ghada Sahbeni[3]

[1] University of Chinese Academy of Sciences, Beijing 100039, China.
[2] Key Laboratory of Ecological Safety and Sustainable Development in Arid Lands, Northwest Institute of Eco-Environment and Resources, Chinese Academy of Sciences, Lanzhou, China. ngabire01@mails.ucas.ac.cn, wt@lzb.ac.cn, xianxue@lzb.ac.cn, liaojie@lzb.ac.cn, hch@lzb.ac.cn, duanhanchen09@163.com , songxiang@lzb.ac.cn
[3] Department of Geophysics and Space Science, Eötvös Loránd University, Pázmány Péter stny. 1/A, Budapest 1117, Hungary; gsahbeni@caesar.elte.hu

* Correspondence: liaojie@lzb.ac.cn; Tel.: +8613321208515

Abstract: Desertification is a global environmental and socio-economical issue threatening humanity's survival and development. The Shiyang River Basin ecosystem is vulnerable and prone to desertification. In addition, establishing the quantitative analysis of desertification driving factors and understanding their relative contribution, separately or combined, is still an unresolved problem. The present study applied geographic information system (GIS) techniques and a geographic detector model to quantify desertification spatial extent and driving mechanisms. This research utilized Fractional Vegetation Cover (FVC) to elucidate desertification spatial heterogeneity. The 30 years Coefficient of Variation (CV) of the Normalized Difference Vegetation Index (NDVI) was a dependent variable and indicator of ecosystem terrestrial conditions; Elevation, near-surface air temperature, precipitation, wind velocity, land cover change, soil salinity, road buffers, waterway buffers, and soil types were independent variables. The results showed that 89.41% of the total area is under desertification risk, where 20.99% is extremely desertified, 34.45% is severely desertified, 12.05% is moderately, and 21.92% is slightly desertified. The results from the Geodetector model showed that Power Determinant (PD) values ranged between 0.004 and 0.270. Elevation and soil types had the highest contributing factors with PD values of 0.270 and 0.227, whereas precipitation, soil salinity, the buffer of the waterway, and wind velocity played a moderate role with PD values of 0.146, 0.117, 0.107, and 0.071. Near-surface air temperature, road buffer, and land cover dynamics exhibited lower impact with PD values of 0.028, 0.013, and 0.004. In most cases, investigating the interaction between driving factors resulted in a mutual or non-linear enhancement. There was an apparent linear and mutual enhancement between elevation and soil salinity, precipitation, and soil types with values of 0.3513, 0.3232, and 0.3204, respectively. In addition, there was a mutual enhancement between soil salinity and soil types with a value of 0.2962. On the other hand, a non-linear enhancement was observed between Elevation and near-surface air temperature (0.3116), Elevation and Land cover dynamics (0.2759), soil types and near-surface air temperature (0.2687), land cover dynamics and soil types (0.234), precipitation and near-surface air temperature (0.2248), precipitation and wind velocity (0.2248), and between land cover dynamics and precipitation (0.223). This research revealed irrefutable evidence that environmental factors might be the primary drivers of ecosystem disturbance, provided the basis for the environmental footprint of desertification mechanism, and might be a cornerstone for future policy on ecological restoration sustainability in the Shiyang River Basin.

Keywords: Desertification, Geographical Detector Model; Google Earth Engine; Driving factors; The Shiyang River Basin

 doi:10.20944/preprints202304.0197.v1

1. Introduction

Desertification is a global drylands threat characterized by the gradual degradation of soil productivity, loss, and thinning of vegetation cover in arid and semi-arid regions[1-3]. Desertification endangers the well-being of billions of people, driving species to extinction, intensifying climate change, and contributing to mass human migration and increased social conflicts [4, 5]. Abnormal and persistent climate change, geomorphological processes, and geographical location are the crucial natural factors of desertification, while demographic pressure and intensive agro-pastoral and unregulated economic activities are leading anthropogenic sources of eco-environment decline in dryland zones[6-8]. Desertification threatens a quarter of the land surface and 10 to 20% of drylands, affecting 250 million people in developing countries[9, 10]. In addition, more than 12 million hectares of farmland are lost yearly due to only desertification and drought, with an approximate yearly loss of 20 million tons of crops supposedly produced by degraded lands[11]. South and East Asia, Southern Africa, the Citrum of Sahara, the Middle East, Latin America, the Caribbean, and western and southwestern parts of the United States of America are the most damaged areas by desertification [11-14].

China experienced multiple arid phases throughout the Quaternary period and intermittence in desertification degrees in the past five decades[15]. This phenomenon attracted scientists to understand these changes' causes and historical trends due to their potentially colossal significance for the global ecology and food supply[7, 16-20]. However, since the 1950s, desertification has increased in China, peaking between the 1970s and early 1980s, then later started ecosystem rehabilitation projects[15]. Particularly the Shiyang River Basin, as a pivotal in natural resource reserves in the Hexi Corridor zone, has also been subject to extreme natural and excessive anthropogenic pressures leading to rapid ecological deterioration and desertification at an unprecedented rate [21, 22]. For example, temperature increases and reduced glacial meltwater in the Qilian Mountains have led to a water supply shortage for the past few decades[23]. In addition, soil salinization and human economic activities, such as the overexploitation of groundwater resources for irrigation works, resulted in the depletion of vegetation cover and desertification at an unprecedented rate, particularly in the lower reaches[24, 25].

Various scientific approaches, such as biophysical and socio-economic data collection and numerical modeling techniques, have been used to understand desertification at different spatiotemporal scales [26-30]. However, previous research highlighted the primordial role of analyzing biological indicators to describe ecosystem functioning as a proxy for better assessing and monitoring land degradation and desertification [31].The earth observation approach provides a state-of-the-art technique for assessing and monitoring multi-temporal and multiscale ecosystem dynamics. For example, Remote Sensing and GIS extensively serve to understand soil properties, the dynamics, and the vegetation response to climate fluctuations and human activities in different landscape types worldwide[32-41]. Consequently, this technique can provide a comprehensive observation of dryland areas, help to ensure and set up fact-based policy and management system, provide early warnings over potential disasters and prevent the unsustainable use of ecosystem goods and services[42, 43]. Several studies revealed some Remote Sensing indicators suitable for dryland observation, and few approaches and numerical models had been developed for qualitative and quantitative measurement. These measures include biological indicators such as vegetation greening trend patterns and physical indicators such as top-layer soil properties, landscape change, etc. [44-50].

Although these studies empirically attributed climate change and human activity as factors responsible for the observed changes in desertification, they merely relied on

Preprints (www.preprints.org) | NOT PEER-REVIEWED | Posted: 11 April 2023 doi:10.20944/preprints202304.0197.v1

inferences based on correlations between trends[51-54]. In addition, these studies only focused on elucidating the status and dynamics of desertification[55-58]. However, quantitative analysis of each driving factor's contribution is still unclear and must be solved to facilitate the implementation of target 15.3 of the Sustainable Development Goals (SDG) to reach zero land degradation by 2030. Moreover, existing statistical approaches to assess influencing factors for vegetation cover change and greening patterns, such as correlation, regression, factor, and geographic regression analyses, merely involve assumptions regarding data but fail to shed light on the interaction between factors and are hindered mainly by multicollinearities among influencing factors[50].

On the other hand, the Geographic Detector Model (GeoDetector) does not operate based on linear hypothesis, rendering it a simple and strait application [59]. More importantly, this approach works with categorical and continuous variables and all data types[60]. In addition, Geodetector can explicitly determine interdependence between dependent variables without restricting multicollinearities[61]. Therefore, this study will combine human and environmental factors data to understand the desertification driving mechanism through quantitative analysis of interactive effects between environmental and anthropogenic factors in the Shiyang River Basin.

2. Materials and Methods

2.1. Study area description

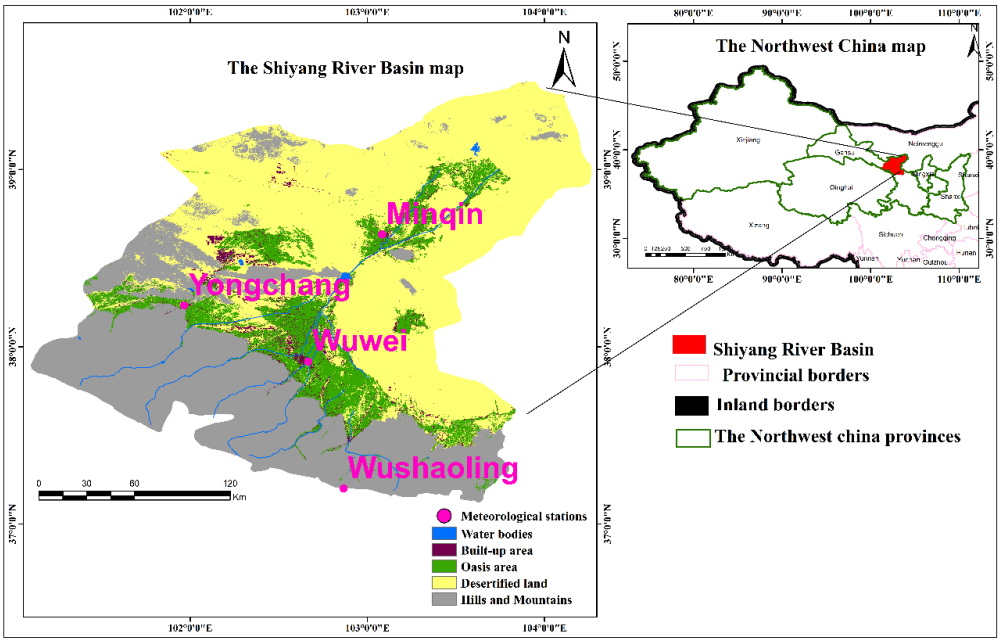

Figure 1 The geographic location of the study area: The Shiyang River basin

The Shiyang River Basin lies between 101°41'-104°16'E and 36°29'-39°27'N, in the east of the Hexi Corridor in Gansu Province, west of Wushaoling and North of the Qilian Mountains, covering a total area of 41,600 square kilometers [62]. High mountains in the South characterize its topography with altitudes ranging from 2000 to 5000 meters; the central plain corridor area covering the east of Longshou Mountain extends to the remnants of the Hanmu Mountain, Hongya Mountain, and Aragua Mountain with the altitude ranging from 1400-2000 m [63]. The North Basin includes the Minqin Basin, Jinchuan, and Changning Basin, ranging from 1300 to 1400 m altitude [64]. In ad-

 doi:10.20944/preprints202304.0197.v1

dition, the basin can be divided into four geomorphological units: the Qilian Mountains in the South, the Central Corridor Plain Area, the Northern Low Mountain and Hilly Area, and the Desert Area [65]. The Shiyang River Basin is deep in the continent's hinterland and belongs to the continental temperate arid climate, distinct by extreme sun radiation, sufficient sunshine, significant temperature difference, little precipitation, intense evaporation, and dry air [66].

The watershed runs from the South to the North, roughly divided into three climatic zones: Alpine, semi-arid, and semi-humid zone of the southern Qilian Mountains at the altitude of 2000 and 5000 m, with annual precipitation of 300 to 600 mm, with annual evaporation of 700 to 1200 mm, and drought index ranging between 1 and 4. The central corridor plain with altitude ranging between1500 to 2000 meters, annual precipitation of 150 to 300 mm, annual evaporation of 1300 and 2000 mm, and drought index between 4 and 15. The warm and dry Northern part comprises all of Minqin, North of Gulang, Northeast of Wuwei, and North of Longshou Mountain in Jinchang City. The altitude is between 1300 and 1500 m, the annual precipitation is less than 150 mm, and the North of Minqin is close to the edge of the Tengger Desert. The annual rainfall in the marginal zone is around 50 mm, yearly evaporation ranges between 2000 and 2600 mm, and the drought index ranges between 15 to 25 [67]. The Shiyang River basin comprises the Dajing River, Gulang River, Huangyang River, Zamu River, and Jinta River from east to West [68].

The administrative division of the basin includes Gulang County, Liangzhou District, Minqin County, Tianzhu County of Wuwei City, part of Yongchang County, Jinchuan District of Jinchang City, Sunan Yugur Autonomous County, and Shandan of Zhangye City[68]. The study area is one of the fast-growing industrial and agricultural activities among other regions in the Hexi corridor [69], with a total population of 2.2689 million according to The 2003 Census, where the urban population is 733,900 people, the rural population is 1.535 million people, and the urbanization rate is 32.35% [70, 71].

Preprints (www.preprints.org) | NOT PEER-REVIEWED | Posted: 11 April 2023 doi:10.20944/preprints202304.0197.v1

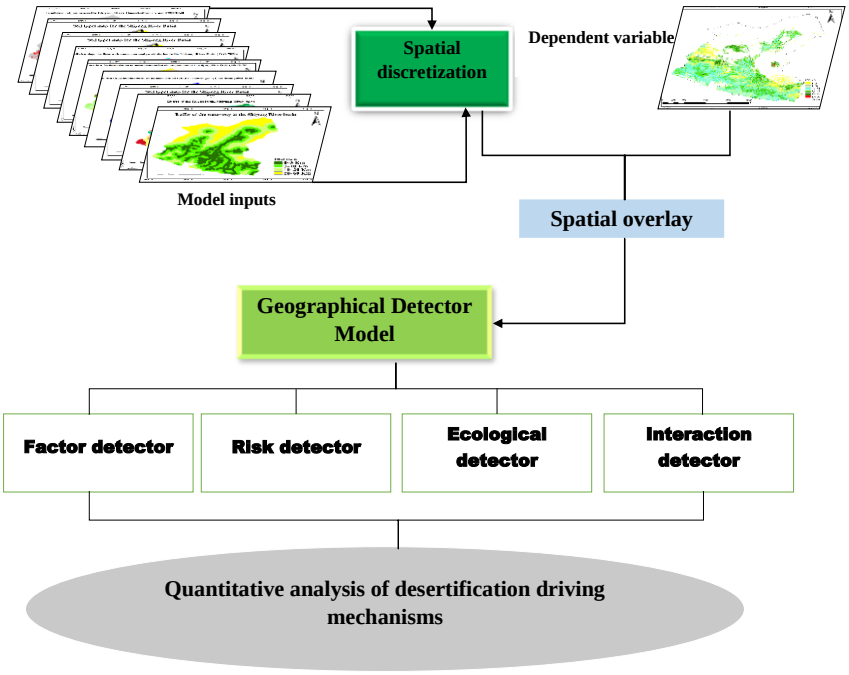

Figure 2 Technological roadmap for the study

1.2. Model inputs parameters

This study considered the 30 years Coefficient of Variation (CV) of the Normalized Difference Vegetation Index (NDVI) as a dependent variable and indicator of ecosystem terrestrial conditions; on the other hand, Elevation (DEM), near-surface air temperature, precipitation, wind velocity, land cover change, soil salinity, road buffers, waterway buffers, and soil types were independent variables and proxies for assessing and quantifying driving factors associated to land degradation and recovery in the Shiyang River Basin Figure 3.

Terrain analysis is crucial for modeling environmental systems [72]. This study chose DEM as a land degradation driving factor due to topographic complexity and elevation gradient effect on the regional microclimate along the Qilian Mountains [73, 74]. DEM data were downloaded from Google Earth Engine (GEE), and a detailed explanation of the algorithms used for terrain data processing and visualization can be found in the paper published by [75]. Unfortunately, demographic growth and structure, livestock, and carbon emission data are not available for Land cover change, but Hydrology, buffer roads, and waterways served as alternative auxiliary variables to assess the anthropogenic factors of land degradation. During data processing, roads, buildings, and waterways in the Shiyang River Basin were vectorized based on Google Earth imagery; then, buffers were analyzed using the Euclidean distance function on QGIS 3.24.0. The smaller the Euclidian distance is to roads and urban settlements, the higher the human impact on the Land; the smaller the distance to water, the higher the soil moisture; hence, the lesser susceptibility to land degradation. Data from land cover dynamics were also used as a proxy to highlight both the climate effect and the established land-use policy's contribution to ecological status. Data were obtained from a Landsat 8 OLI imagery, and the map was produced following the China landcover classification system and Land Use Remote Sensing Mapping Classification system [76].

Preprints (www.preprints.org) | NOT PEER-REVIEWED | Posted: 11 April 2023 doi:10.20944/preprints202304.0197.v1

Soil salinization significantly threatens soil's geochemical properties, especially in dryland areas [77]. Moreover, many studies proved the relationship between soil salinization, climate change, soil fertility loss, and ecosystem deterioration [78]. In this study, soil salinity content information is retrieved from a Landsat-based map produced using a multiple linear regression model based on the work of [79]. Equation (1) presented below is used to retrieve soil salinization.

$$\mathbf{EC\ (dS/m)} = -\mathbf{0.8963161} + \mathbf{5.5292290} \times (\mathbf{B_8}) + \mathbf{2.7199391} \times (\mathbf{G} \times \mathbf{SWIR_1}) + \mathbf{2.3664955} \times (\mathbf{B} \times \mathbf{SWIR_1}) + \mathbf{2.7685607} \times \mathbf{SI_5} \quad (1)$$

Where EC is Electrical conductivity in dS/m (decisiemens per meter), B_8 is the Panchromatic band, G is the Green band, $SWIR_1$ is shortwave infrared1, and SI_5 stands for salinity index 5.

Gridded annual mean precipitation, wind velocity, and near-surface air temperature with 1 km resolution from 1990 to 2021 were generated through spatial interpolation based on daily data from National Meteorological Stations and downloaded from the Cloud Platform of the Chinese Academy of Sciences (http://www.resdc.cn). 1 km resolution soil types data were collected from the Cold and Arid Regions Science Data Center at http://westdc.westgis.ac.cn/. In addition, growing season median vegetation data were generated in the cloud and downloaded from Google Earth Engine (GEE).

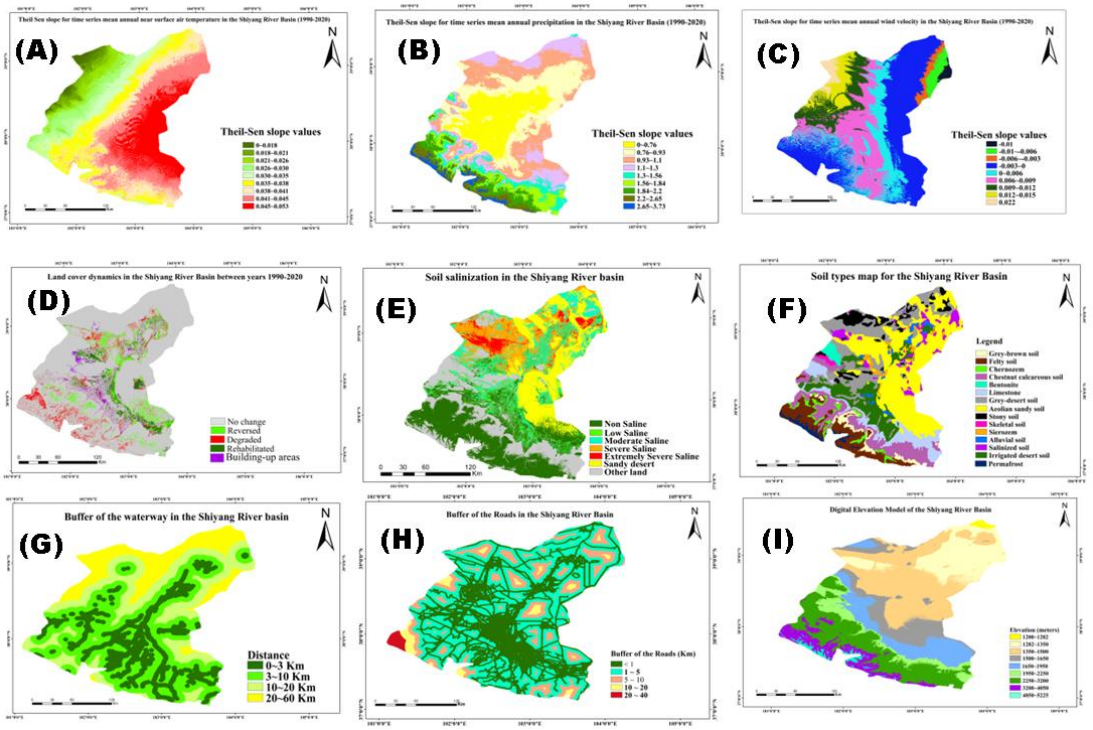

Figure 3 Model inputs: A-temperature, B-precipitation, C-wind velocity, D-land cover change, E-soil salinization, F-soil types, G-buffer to waterways, H-buffer to roads, I- Elevation.

1.3. Geographic detector model

The geographical detector model or GeoDetector is a tool that measures stratified spatial heterogeneity (SSH), generating a spatial differentiation between intra-strata and inter-strata phenomena while elucidating the validity of their spatial partition and driving factors [59]. GeoDetector measures and detects the SHH among data, then test the coupling between two variables, X and Y, based on their respective SSH without assuming their linearity, and finally explores the interaction between the two explanatory variables Xi and Xj in response to variable Y without any predefined form of interaction[80]. Stratified

Preprints (www.preprints.org) | NOT PEER-REVIEWED | Posted: 11 April 2023 doi:10.20944/preprints202304.0197.v1

spatial heterogeneity gained a broad application, particularly in public health, environment, ecology, and forestry studies[81-83].

This universal tool has various applications and provides objective and accurate evaluation as it is insensitive to the results interference due to human errors [84]. In recent years, more researchers have investigated the adverse impacts of anthropogenic and natural-induced processes on desertification, suggesting a more comprehensive approach to thoroughly understand desertification's fundamental drivers [6, 85].

The proposed method can numerically and quantitatively differentiate between independent variables and outline the interaction between two dependent variables. In addition, it can perform a spatial heterogeneity analysis for negatively distributed variables when independent variables are quantifiable [86]. Therefore, variables convert into discrete intervals, also known as discretization, based on the quantile and equal spacing classification by minimizing the variance within the interval and maximizing the variance between intervals [87]. The GeoDetector model comprises a Risk, Factor, Ecological, and Interaction detector [88]. Details about the conceptual basics of Geographic Detectors are illustrated in Table 2, while more information can be found in the R package, along with its manual and study case, at CRAN - Package GD (r-project.org).

1.3.1. Factor detector

The interoperation of different factors' impact on regional heterogeneity is based on spatial variance analysis on geographical strata following the model proposed by[89]. The association between spatial variance and a geographical detector model can be expressed using equation (2).

$$PD = 1 - \frac{\sum_{h=1}^{L} \sum_{i=1}^{N_h} (y_{h1} - \bar{y}_h)^2}{\sum_{i=1}^{N} (y_i - \bar{x})^2} = 1 - \frac{\sum_{h=1}^{L} N_h \sigma_h^2}{N\sigma^2} \qquad (2)$$

PD is the power determinant based on the spatial heterogeneity of the study object. L is the strata subdivisions of the study denoted by h=1,…, L. σ^2 and σ^2_h are the units variances [90]. N and N_h are the study area units, and h is the strata. The PD interval varies between 0 and 1, i.e. [0,1], meaning that PD=0 if the determinant is utterly unrelated to the risk, whereas PD=1 when the determinant controls the risk.

The spatial discretization optimization aims to identify the optimum spatial scale for the spatial stratified heterogeneity analysis over different scales indicating that the obtained PD of all explanatory variables with their respective spatial discretization parameters at various scales must be compared with corresponding spatial scales to investigate their relationships. Optimizing the spatial discretization and scale requires a delicate selection of discretization methods and break numbers for each continuous geographical variable. The best parameter combination is determined by the PD value specified with the factor detector. During the PD values computation, a set of discretization methods and break numbers are provided for each variable[87, 91]. Even though the combination is optional, spatial discretization covers almost all available choices where break numbers can be integer sequences depending on observations and practical requirements. A parameter combination with the highest PD is the best choice of a continuous variable for spatial discretization as it presents the variable's highest importance in stratified spatial heterogeneity[92, 93].

Preprints (www.preprints.org) | NOT PEER-REVIEWED | Posted: 11 April 2023 doi:10.20944/preprints202304.0197.v1

1.3.2. Risk detector

The risk detector can be applied to test the significant difference among mean values of subregions classified following categorical or stratified variables [86, 87]. The expression for Risk Detector is given by equation (3).

$$t_{\bar{Y}_\eta} + \bar{x}_1 = \frac{(\bar{Y}_\eta - \bar{Y}_k)}{\sqrt{\frac{s_\eta^2}{N_\eta} + \frac{s_k^2}{N_1}}} \quad (3)$$

$\bar{Y}_\eta$ and $\bar{Y}_k$ are the mean values of observations within sub-regions η and k. s^2_η and s_k^2 represent sample variance, while N_η and N_k stand for observations number. The statistics for this factor follow the Student's distribution table; hence the degree of freedom can be expressed using equation (4).

$$df = \frac{\left(\frac{s_\eta^2}{N_\eta} + \frac{s_k^2}{N_k}\right)}{\left[\frac{1}{N_\eta - 1}\left(\frac{s_\eta^2}{N_\eta}\right)^2 + \frac{1}{(N_k - 1)}\left(\frac{s_k^2}{N_k}\right)^2\right]} \quad (4)$$

The Student-t distribution table can test the null hypothesis H0, presented by equation (5), at a 0.05 significant level.

$$H_0: \bar{Y}_\eta = \bar{Y}_k \quad (5)$$

1.3.3. Ecological detector

An ecological detector is a robust tool employed to test explanatory variables' efficiency by confirming whether one factor, X_1 has a higher impact over another X_2 [87], as expressed in equation (6).

$$\mathbf{F} = \frac{\mathbf{N_u(N_v - 1)} \sum_{\mathbf{j=1}}^{\mathbf{M_u}} \mathbf{N_u \sigma_{u,j}^2}}{\mathbf{N_v(N_u - 1)} \sum_{\mathbf{j=1}}^{\mathbf{M_v}} \mathbf{N_v \sigma_{v,j}^2}} \quad (6)$$

N_u and N_v stand for observations number. M_u and M_v are the sub-regions numbers, $\sum_{j=1}^{M_u} \boldsymbol{N_u \sigma_{u,j}^2}$ and $\sum_{j=1}^{M_v} \boldsymbol{N_v \sigma_{v,j}^2}$ are variance sums within sub-regions of variables u and v. As a result, with a given significance level, the null hypothesis.

$\mathbf{H_0} = \sum_{j=1}^{M_u} \boldsymbol{N_u \sigma_{u,j}^2} = \sum_{j=1}^{M_v} \boldsymbol{N_v \sigma_{v,j}^2}$ can be tested with the F-distribution table.

The systematic computation and visualization of the optimal geographical detector model can be executed in R using the GD software package. An extended presentation of the package can be found in R Documentation.

1.3.4. Interactive factor

Many factors influence the spatial heterogeneity of Y. The interaction between every two factors may enhance, weaken, or stay intact based on the spatial heterogeneity of Y [59]. For instance, the power of the determinant of factors X_i and X_j toward Y were calculated,

Preprints (www.preprints.org) | NOT PEER-REVIEWED | Posted: 11 April 2023 doi:10.20944/preprints202304.0197.v1

then X_i and X_j overlaid to form a new stratum. Figures 4 and 5 show that the newly formed stratum allows the determination of PD of interaction between X_i and X_j. The assessment of the interactive influence between the two factors is illustrated in Table 1. A thorough description of GeoDetector software and its operating mode can be found in [94].

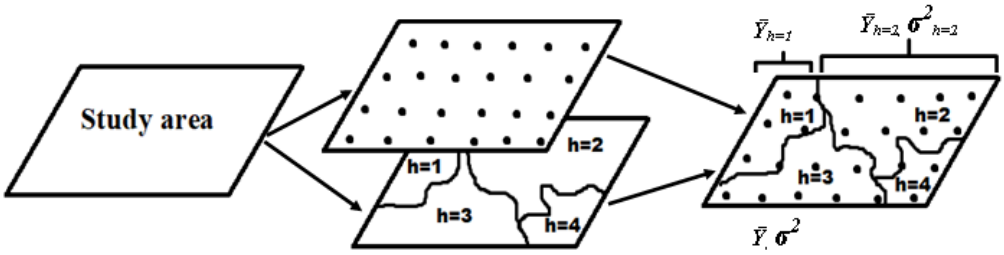

Figure 4 The basic concept of Geographic Detector: The strata of Y were formed by laying Y over X; the PD interval varies from [0,1], and the PD reflects X's influence on Y's spatial heterogeneity. The larger the PD is, the more significant the Impact of X is [80].

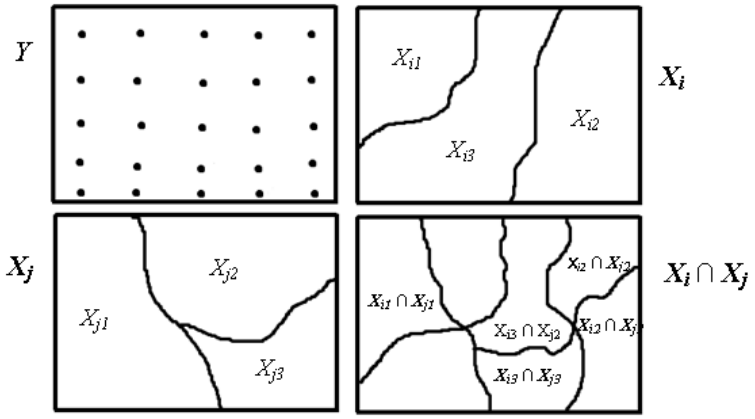

Figure 5 Detection of interaction between different factors. [80]

Table 1 Interaction relationship between two variables and their impact categories. Min(PD(Xi), PD(Xj)) is the minimum of PD(Xi) and PD(Xj), while Max(PD(Xi), PD (Xj)) is the maximum of PD(Xi) and PD(Xj) [95].

Demonstration of interaction relationship	Factor interaction type
$PD\ (Xi \cap Xj) < Min\ (PD\ (Xi), PD\ (Xj))$	The factors weakened & non-linear
$Min\ (PD\ (Xi), PD\ (Xj)) < PD\ (Xi \cap Xj) < Max\ (PD\ (Xi)), PD\ (Xj))$	The factors weakened & univariate
$PD\ (Xi \cap Xj) > Max\ (PD(Xi), PD\ (Xj))$	The factors enhanced & bivariate
$PD\ (Xi \cap Xj) = PD\ (Xi) + PD\ (Xj)$	The factors are independent
$PD\ (XiXj) > PD\ (Xi) + PD\ (Xj)$	The factors are enhanced & non-linear

Table 2 Summary for conceptual basis of Geographic Detectors [92].

Type of Detector	*Conceptual explanation*

Preprints (www.preprints.org) | NOT PEER-REVIEWED | Posted: 11 April 2023 doi:10.20944/preprints202304.0197.v1

Factor detector	This method used the Power Determinant (PD) to evaluate the Impact of Land-cover, DEM, Soil salinization, Land surface temperature, water buffer, and road buffer on the spatial distribution of FVC. In addition, F-test was performed to determine whether each subregion's accumulated variance differed significantly from the variance of the whole region.
Risk detector	It compares the difference in average FVC between subregions strata. The t-tests were used to identify whether the FVC among different sub-regions is significantly different.
Ecological detector	It evaluates whether the impact of environmental and human factors on FVC is significantly different. The F-test was applied to compare the variance calculated in the subregion attributed to one triggering factor with the variance attributed to another.
Interaction detector	It evaluates the combined impact of two factors on desertification and their respective independent contribution. In addition, it assesses whether the combined factors weaken or enhance each other or independently influence desertification magnitude. The process comprises seven parts: Enhance, Enhance-bi, Enhance-nonlinear, Weaken, Weaken-uni, Weaken-nonlinear, and Independent.

1.4. Grading standards for desertification

Many studies have investigated the link between desertification and vegetation density loss, proving that the less Land is covered by vegetation, the more its susceptibility to desertification [96]. Thus, spectral indices such as the Normalized Difference Vegetation Index (NDVI), Leaf Area Index (LAI), Modified Soil Adjusted Vegetation Index (MSAVI), Net Primary Productivity (NPP), Vegetation Rain Use Efficiency (RUE), Fractional Vegetation Cover (FVC), and some others used in Remote Sensing based approaches for assessing land degradation and desertification and land degradation in general [97]. Among these indices, FVC represents a key phenotypic parameter in agriculture, forestry, and ecology in particular [98], which justifies why the fractional vegetation cover is more efficient for quantitative analysis of land degradation degree in this study, assuming that the smaller the mean annual FVC, higher is desertification vulnerability, and vice versa [99]. A cloud-free mosaic of Landsat 8 TOA collection images was acquired and used to calculate the mean annual NDVI on the GEE environment cloud. The extraction of growing season mean FVC was performed to minimize errors caused by bare Land and extremely vegetated zones [100]. The FVC was determined using equation (7).

$$FVC = \frac{(NDVI - NDVI_{soil})}{(NDVI_{veg} - NDVI_{soil})} \quad (7)$$

Preprints (www.preprints.org) | NOT PEER-REVIEWED | Posted: 11 April 2023 doi:10.20944/preprints202304.0197.v1

$NDVI_{soil}$ is the NDVI of the bare Land with a value of 0.05 in arid zones, usually consisting of sparse shrubland and pure barren Land. $NDVI_{veg}$ stands for the NDVI in pure vegetation, roughly estimated to be 0.6 in arid zones [101]. Grading the desertification follows the previous study standards [95, 102]. Detailed information is presented in Table 3.

Table 3 Classification of desertification degree in the Shiyang River basin

Intensity	FVC Range	Surface feature characteristics
No desertification	> 0.5	Grassland, farmland, forest.
Slight desertification	0.4–0.5	Meadow, grassland, farmland
Moderate desertification	02–0.4	Less dense vegetation
Severe desertification	0.1–0.2	Patches of vegetation across sandy and saline lands
Very severe degraded	< 0.1	Shifting sand, sandy gravy land, salt scald, and bare lands

3. Results

3.1. Spatial distribution of desertification and land cover dynamics in the Shiyang River Basin

Figure 6 shows desertification's spatial distribution in the Shiyang River Basin based on mean annual fractional vegetation cover. Higher values were recorded in the alpine forest and meadow at the top of the Qilian mountains, which gradually decreased in the subalpine shrub vegetation zone along the mountain ridge towards the basin's middle reach. FVC ranges between 0.1 and 0.2 in steppe vegetation, covering parts of mountainous areas in the upper reach and some parts of the middle and lower reach. Farmland areas in Gulang, Lianzhong, Wuwei, Yongchang districts, and Minqin had FVC values greater than 0.4. Regarding desertification levels, 20.99% are extremely desertified, 34.45% are severely desertified, 12.05% are moderately desertified, 21.92% are slightly desertified, and only 9.35% are not desertified.

Preprints (www.preprints.org) | NOT PEER-REVIEWED | Posted: 11 April 2023 doi:10.20944/preprints202304.0197.v1

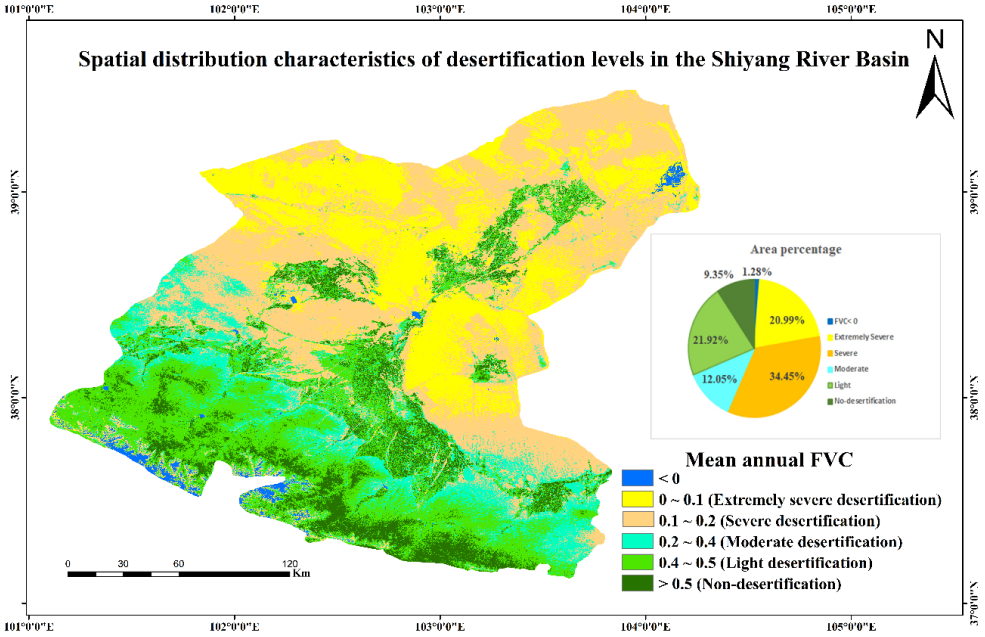

Figure 6 Spatial distribution of desertification levels in the Shiyang River basin.

3.2. Quantitative analysis of factors governing the ecological status and dynamics in the Shiyang River Basin

As shown in Fig 7, the analysis of power determinant (PD) values of all studied driving factors ranged between 0.004 and 0.270. Elevation and soil types had the highest contributing factors with PD values of 0.270 and 0.227, whereas precipitation, soil salinity, buffer to the waterway, and wind velocity played a moderate role with PD values of 0.146, 0.117, 0.107, and 0.071. On the other hand, near-surface air temperature, road buffer, and land cover dynamics exhibited lower Impact with PD values of 0.028, 0.013, and 0.004. In most cases, investigating the interactive effects of driving factors resulted in a mutual or nonlinear enhancement of PD values interaction between elevation and soil salinity was the highest with a value of 0.3513. More importantly, there was an apparent mutual enhancement between elevation and soil salinity, precipitation, soil types, and wind velocity with values of 0.3513, 0.3232, 0.3204, and 0.2981. In addition, there was also a mutual enhancement in soil salinity with soil types, water buffers, wind velocity, and near-surface air temperature with values of 0.2962, 0.1924, 0.1881, and 0.1586.

Preprints (www.preprints.org) | NOT PEER-REVIEWED | Posted: 11 April 2023 doi:10.20944/preprints202304.0197.v1

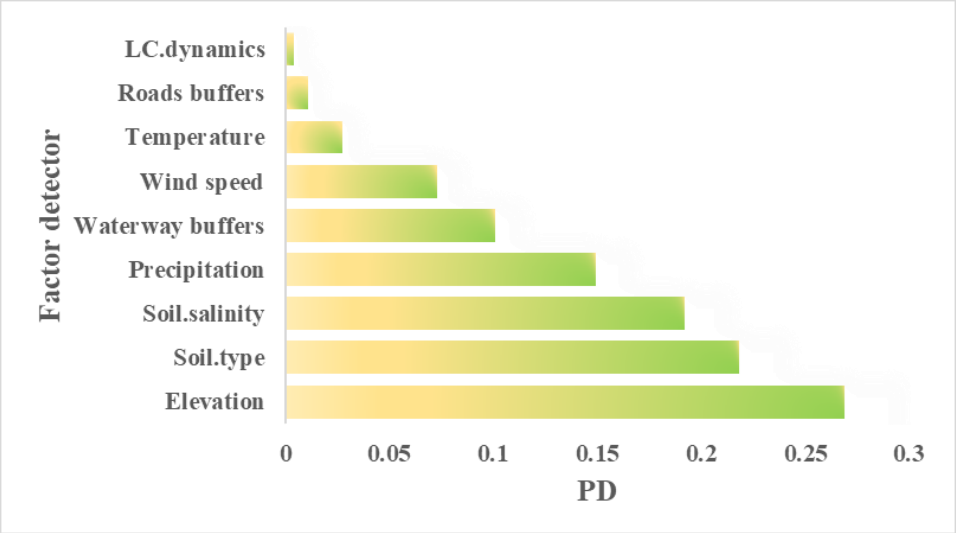

Figure 7 Geographical detector-based explanatory variables of driving factors of desertification in the Shiyang River basin: Contribution of a single variable on FVC changes investigated by factor detector.

3.3. Environmental risk detection of desertification in the Shiyang River Basin

Fig 8 illustrates that the risk detector results highlight the linear or non-linear change among strata. For example, waterway buffers and elevation influence on NDVI variance followed a linear pattern. There is a clear relationship between vegetation change dynamics, elevation gradient, and distance to the waterway. Temperature, precipitation, and soil salinity also followed the same pattern but with some minor exceptions that may be related to irrigation activities in lower reaches. Grey-brown and chestnut calcareous soil in Qilian Mountains grassland zones were the most susceptible to change, followed by chernozem, felty soil, and permafrost, all located in Qilian Mountains meadow vegetation. A remarkable variance in permafrost and irrigated sandy soil indicated that glacier thaw impacted soil conditions in the upper reaches and water resources availability in the lower reaches. No apparent patterns existed between vegetation dynamics, wind velocity, and road buffers.

Preprints (www.preprints.org) | NOT PEER-REVIEWED | Posted: 11 April 2023 doi:10.20944/preprints202304.0197.v1

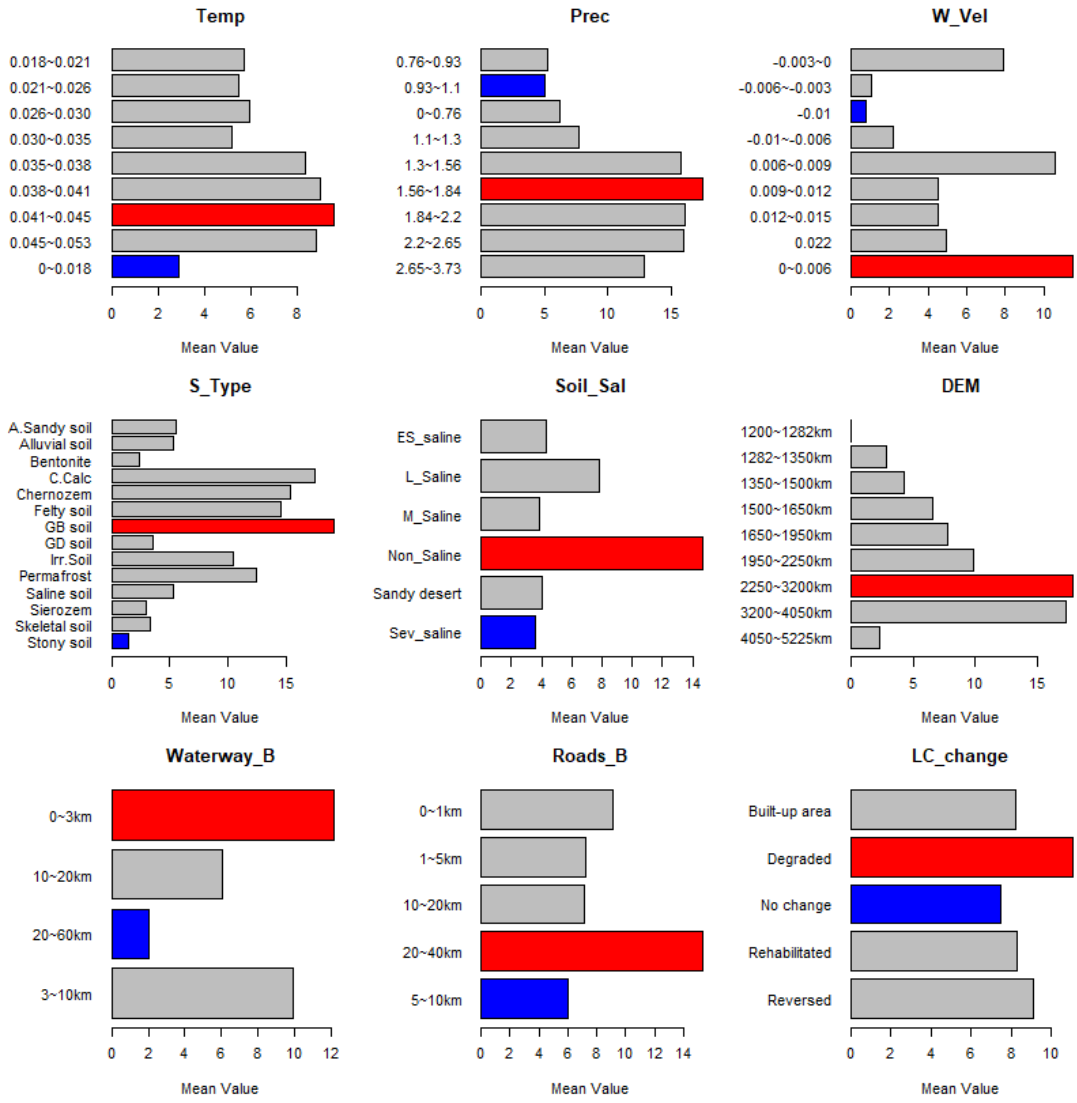

Figure 8 Influence of factors' different strata on the magnitude of the increase in the NDVI coefficient of variation (L: Low, M: Moderate, Dev: Severe, ES: Extremely Severe, A.Sandy soil: Aeolian sandy soil, GB soil: Grey-brown soil, GD soil: Grey-desert soil, Irr soil: Irrigated desert soil

3.4. Interaction between ecosystem's driving factors in the Shiyang River basin

Table 4 and Fig 9 illustrate the evaluation of the interaction between factors of desertification in the Shiyang River Basin. As emphasized in previous studies, this kind of interaction is not a simple linear summation, yet it evaluates whether two influencing factors are independent or either enhance or weaken each other. Most driving factors enhanced each other, meaning the interactive PD values resulted in a higher value than a single factor. For example, a non-linear enhancement was observed between Elevation and near-surface air temperature, Elevation and Land cover dynamics, soil types and near-surface air temperature, land cover dynamics and soil types, precipitation and near-surface air temperature, precipitation and wind velocity, and between land cover dynamics and precipitation. Their values are 0.3116, 0.2759, 0.2687, 0.234, 0.2248, 0.223, and 0.1544. The fact that

 doi:10.20944/preprints202304.0197.v1

some factors enhanced each other and others had a non-linear enhancement among studied driving factors implies that a single driving factor can not define or justify the status and dynamics of ecological functioning in the Shiyang River Basin.

Table 4 Correlation matrix for interaction detector obtained from a geographical detector-based explanatory variable (Wind. V = wind velocity, B.water= waterway buffers, Temp= near-surface air temperature, ST= soil type, SS= soil salinity, Prec= precipitation, LC.dyn= land cover change, Elv= Elevation)

	Wind.V	B.water	Temp	ST	SS	Prec	LC.dyn	Elv
B.water	0.1517							
Temp	0.1143	0.1455						
ST	0.265	0.2513	0.2687					
SS	0.1881	0.1924	0.1586	0.2962				
Prec	0.223	0.2113	0.2248	0.2748	0.2431			
LC.dyn	0.0776	0.1126	0.038	0.234	0.1208	0.1544		
Elv	0.2981	0.2889	0.3116	0.3204	0.3513	0.3232	0.2759	
B.Roads	0.0859	0.1115	0.0484	0.235	0.1254	0.1654	0.0186	0.2762

Preprints (www.preprints.org) | NOT PEER-REVIEWED | Posted: 11 April 2023 doi:10.20944/preprints202304.0197.v1

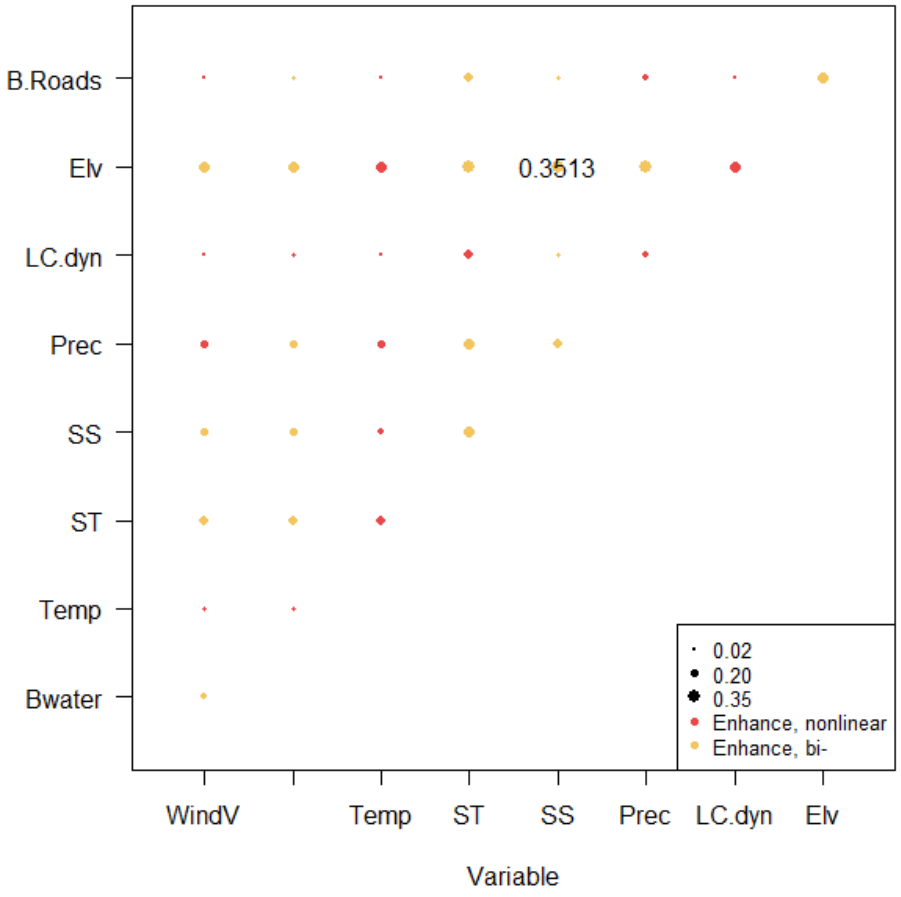

Figure 9 Interaction detector obtained between explanatory variables

4. Discussion: Understanding factors' interaction effect on desertification in the Shiyang River Basin

Many studies have addressed natural and anthropogenic factors' role in land degradation or recovery, particularly in dryland zones[50, 52, 102]. Previous research have applied GIS techniques to analyze the spatiotemporal dynamics of desertification in the Shiyang River Basin and they highlighted the leading driving causes, such as climatic fluctuation, soil salinization, and water resources overexploitation [47, 79, 103, 104]. However, the quantitative analysis of desertification driving factors and understanding their relative contribution, separately or combined, is still an unresolved problem. Therefore, as shown in Fig 2, this study discusses and provides a scientific basis for understanding the relative importance and interaction between factors towards desertification. Fig 7 also illustrates the contribution of each factor where PD values varied as follows in decreasing order: Elevation > soil types > soil salinity > wind velocity > temperature > precipitation > waterway buffers > road buffers > and land cover dynamics.

Elevation gradient plays a key factor for both climate and vegetation spatial heterogeneity across the Shiyang River Basin, Fig 8. Research revealed that the upstream receives sufficient water resources from precipitation and glacier thaw, rendering this sub-region suitable for forest and grassland growth[105]. In addition, the gradient increase in temperature and evaporation, along with a decrease in rainfall, triggers gradual vegetation covers decline from upstream to lower reaches, rendering the extension of barren Land in lower

 doi:10.20944/preprints202304.0197.v1

reaches [22, 106]. This corroborates the current spatial distribution of desertification levels across the Shiyang River Basin Fig 6, where around 55% of the area of interest is under severe desertification risk, primarily in the basin's middle and lower reaches. However, for the past few decades, anthropogenic activities, namely watershed management and ecological restoration projects through sand fixation projects, have significantly impacted the hydrological regime and spatial distribution of vegetation in the middle and lower reaches[25, 107-109]. As a result, contrarily to the upper areas of the Qilian mountains, vegetation greening patterns depend more on human activities than natural phenomena, as confirmed by recent research [108, 110]. In addition, this suggests that topographic landforms and climate play a significant role in developing geomorphic features in the Shiyang River Basin. Similar findings corroborate previous studies on desertification, aeolian processes, and landforms' response to climate change [96, 111-122].

Besides natural phenomena, anthropogenic activities may worsen or improve the ecosystem, particularly in Drylands. For example, overexploitation of water resources, unconventional mining activities, overgrazing, and many others trigger land degradation, such as soil salinization and desertification in arid and semi-arid regions[123-127]. As shown in Fig 7& 8, soil salinization is one of the leading factors of ecological status in the Shiyang River basin, and its effects on vegetation health were proportional to salt concentration in the soil. These results corroborate previous findings highlighting that soil salinization deteriorated environmental conditions in the Shiyang River Basin, especially in the Minqin oasis[128, 129]. In addition, Optimizing water resources in densely populated zones is challenging for scientists, communities, and policymakers, especially in arid and semi-arid regions [130]. For example, several studies conducted in the Shiyang River basin raised concerns about the correlation between population pressure and water resources shortage as the center of desert expansion in the Shiyang River basin[47, 71, 131, 132]. However, by analyzing road networks and waterway buffers as a proxy for population and water use in the Shiyang River basin, the closer the distance to the waterway, the lower the land degradation risk, Fig 8.

Moreover, there are no clear patterns for road buffers to determine the general trend, which implies that population density and settlement systems do not disturb the ecosystem in the area of interest (Fig 7 & 8). The implication of such results for waterways and road buffers is the irrefutable hypothesis stipulating that ecological deterioration in the Shiyang River basin is no longer related to the human mismanagement of natural resources. As shown in Fig 8, land cover dynamics reveal that desertification is still persistent despite a crucial role played by existing land restoration and watershed management in the Shiyang River Basin. These findings corroborate previous studies emphasizing remarkable gradual ecosystem stability and recovery in the Shiyang River basin during the past few decades despite the odds of climate change, aeolian erosion, some irregularities related to anthropogenic activities, and soil salinization [108, 133].

The linear and mutual enhancement among explanatory variables highlights the uniformity of pattern change relative to ecological status, while a non-linear enhancement status indicates uncertainties in providing a longstanding view that may rate a specific relationship between variables[59]. However, as revealed in previous studies, this relationship does not necessarily implicit a linear summation or interdependence [134-136]. This study revealed that some factors enhanced each other and others had a non-linear enhancement among studied driving factors, implying that a single factor can not define the status and dynamics of ecological functioning in the Shiyang River Basin. Table 4 & Fig 9 illustrate the results of interactions between driving factors. For example, this study showed an apparent linear and mutual enhancement between elevation and soil salinity, elevation~ precipitation, and elevation~soil types, and a mutual enhancement between soil salinity and soil types. On the other hand, a non-linear enhancement was observed between Elevation and near-surface air temperature, Elevation and Land cover dynamics,

 doi:10.20944/preprints202304.0197.v1

soil types and near-surface air temperature, land cover dynamics and soil types, precipitation and near-surface air temperature, precipitation, and wind velocity, and between land cover dynamics and precipitation. This is irrefutable evidence that natural environmental factors may currently be the primary drivers for ecosystem disturbance in the Shiyang River Basin.

These findings shed light on the status and dynamics of land degradation and recovery's main driving factors by highlighting the role of land management, rational water allocation, and conservation measures to reverse land degradation and maintain a sustainable ecosystem despite climate change impacts and water resources shortage in the Shiyang river basin. In addition, by combining human and environmental factors, this research provides scientific evidence of the efficacy of established policies toward reaching LDN and is a cornerstone for future policy on ecological restoration under various natural and anthropogenic scenarios.

5. Conclusions and Prospects

This study used the FVC-based classification method to map desertification spatial heterogeneity across the Shiyang River Basin. In addition, the Geodetector was applied to analyze each desertification driving force's contribution quantitatively. The research combined CV as the dependent variable and multiple environmental and human factors as independent variables.

The findings showed that elevation gradient, soil types, soil salinity, and precipitation play a core role in desertification status and spatial heterogeneity across the Shiyang River Basin. Furthermore, this research revealed that some environmental factors boosted each other. In contrast, others had a non-linear enhancement among studied driving factors, implying that a single parameter can not define the status and dynamics of ecological functioning in the region of interest. This study also demonstrated irrefutable evidence that environmental factors might be the primary drivers for ecosystem disturbance in the Shiyang River Basin and highlighted the role of the established ecosystem rehabilitation policies toward reaching land degradation neutrality as planned. In addition, this research suggests a more advanced eco-environmental protection system against long-term natural factors hindering existing ecosystem restoration, including soil salinization and aeolian erosion, particularly in oasis areas. Moreover, this study is the basis for the environmental footprint of desertification status and a cornerstone for future policy on ecological restoration sustainability in the Shiyang River Basin.

Although Geographical Detector Model is a robust and reliable approach to the quantitative evaluation of drivers and mechanisms of desertification, the model would perform better if more data, including population density, livestock, and carbon footprint, were included; therefore, future studies should consider this remark.

Authors contribution: Conceptualization: Wang, T., **Statistical analysis:** Ngabire, M., **Writing original manuscript:** Ngabire, M.**; Revision of manuscript:** Sahbeni, G., Liao, J., **; Funding acquisition:** Wang, T.

All authors have read and agreed to the published version of the manuscript.

Conflict of interests: The authors declare that they have no known competing financial interests or personal relationships that could have appeared to influence the work reported in this paper.

Acknowledgments: This work was supported by The Ministry of Science and Technology of the People's Republic of China through, The Second Tibetan Plateau Scientific

Expedition and Research Program (STEP), Grant number: 2019QZKK0305, and Science and Technology Department of Ningxia, Grant number: 2020BBF02003.

Data availability: Data will be made available on request.

References

1. Kassas, M., *Desertification: a general review.* J. Arid Environ., 1995. **30**(2): p. 115-128. https://doi.org/10.1016/S0140-1963(05)80063-1
2. Chen, Y. and Tang, H., *Desertification in North China: Background, Anthropogenic impact and Failures in combating it.* Land Degrad. Develop., 2005. **16**: p. 367–376. https://doi.org/10.1002/ldr.667
3. Feng, Q., Ma, H., and Jiang, X., *What Has Caused Desertification in China?* Sci. Rep., 2015. **5**(15998). https://doi.org/10.1038/srep15998
4. Pacheco, F. A. L., Fernandes, L. F. S., Junior, R. F. V., Valera, C. A., and Pissarra, T. C. T., *Land degradation: Multiple environmental consequences and routes to neutrality.* Curr Opin Environ Sci Health, 2018. **5**: p. 79-86. https://doi.org/10.1016/j.coesh.2018.07.002
5. Barbut, M. and Alexander, S., *Land Degradation as a Security Threat Amplifier: The New Global Frontline*, in *Land Restoration: Reclaiming Landscapes for a Sustainable Future*. 2016, Academic Press. p. 3-12.
6. Geist, H. J. and Lambin, E. F., *Dynamic Causal Patterns of Desertification.* BioScience, 2004. **54**(9): p. 817–829. https://doi.org/10.1641/0006-3568(2004)054[0817:DCPOD]2.0.CO;2
7. Wang, F., Pan, X., Wang, D., Shen, C., and Lu, Q., *Combating desertification in China: Past, present and future.* Land Use Policy, 2013. **31**(2013): p. 331-313. https://doi.org/10.1016/j.landusepol.2012.07.010
8. Yue, Y., Geng, L., and Li, M., *The impact of climate change on aeolian desertification: A case of the agro-pastoral ecotone in northern China.* Sci Total Environ, 2013. **859**(2): p. 160126. https://doi.org/10.1016/j.scitotenv.2022.160126
9. Huang, J., Zhang, G., Zhang, Y., Guan, X., and Yun, W., *Global desertification vulnerability to climate change and human activities.* Land Degrad Dev, 2020. **31**(2020): p. 1380–1391. https://doi.org/10.1002/ldr.3556
10. Rafferty, J. P. and Pimm, S. L., *desertification*, in *Encyclopedia Britannica*. 2020.
11. Neary, D. G., *Wildfire contribution to desertification at local, regional, and global scale*, in *Desertification*, V.R. Squires and A. Ariapour, Editors. 2018, Nova Science Publishers, Inc. p. 200-222.
12. Reynolds, J. F., Smith, D. M. S., Lambin, E. F., Turnel, B. L., Mortimore, M., and Batterbury, S. P. J., *Global Desertification: Building a Science for Dryland Development.* Science, 2007. **316**(2007): p. 5826. https://doi.org/10.1126/science.1131634
13. Nickayin, S. S., Coluzzi, R., Marucci, A., Bianchini, L., Salvati, L., Cudlin, P., and Imbreda, V., *Desertification risk fuels spatial polarization in 'affected' and 'unaffected' landscapes in Italy.* Sci Rep, 2022. **12**(747). https://doi.org/10.1038/s41598-021-04638-1
14. Ziadat, F. M., Zdruli, P., Christensen, S., Caon, L., Monem, A., and Fetsi, T., *An Overview of Land Degradation and Sustainable Land Management in the Near East and North Africa.* Sustain. Agric. Res., 2022. **11**(1): p. 11-24. https://doi.org/10.5539/sar.v11n1p11
15. Wang, X., Chen, F., Hasi, E., and Li, J., *Desertification in China: An assessment.* Earth-Sci. Rev, 2008. **88**(3-4): p. 188-206. https://doi.org/10.1016/j.earscirev.2008.02.001
16. Wang, X., Ge, Q., Geng, X., Wang, Z., Gao, L., Bryan, B. A., Chen, S., Su, Y., Cai, D., Ye, J., and Sun, J., *Unintended consequences of combating desertification in China.* Nat Commun, 2023. **14**: p. 1139. https://doi.org/10.1038/s41467-023-36835-z
17. Qi, L., Lei, J., Li, X., Yang, Y., and Feng, W., *China's Combating Desertification: National Solutions and Global Paradigm.* Chin. Sci. Bull., 2020. **35**(6). https://doi.org/10.16418/j.issn.1000-3045.20200427002

18. Hong, J., *Desertification in China: Problems with Policies and Perceptions*, in *China's Environmental Crisis* J.J. Kassiola and S. Guo, Editors. 2010: Palgrave Macmillan, New York. p. 13–40.
19. Kong, Z., Stringer, L., Paavola, J., and Lu, Q., *Situating China in the Global Effort to Combat Desertification.* Land, 2021. **10**(7): p. 702. https://doi.org/10.3390/land10070702
20. Bao, Y., Cheng, L., Yanfeng, B., Yang, L., Jiang, L., Long, C., Kong, G., Peng, P., Xiao, J., and Lu, Q., *Desertification: China provides a solution to a global challenge.* Front. Agr. Sci. Eng., 2017. **4**(4): p. 402–413. https://doi.org/10.15302/J-FASE-2017187
21. Fang, Y., Wang, X., Cheng, Y., and Wang, Z., *Oasis Change Characteristics and Influencing Factors in the Shiyang River Basin, China.* Sustainability, 2022. **14**: p. 14354. https://doi.org/10.3390/su142114354
22. Zhang, Y., Zhu, G., Ma, H., Yang, J., Pan, H., Guo, H., Wan, Q., and Yong, L., *Effects of Ecological Water Conveyance on the Hydrochemistry of a Terminal Lake in an Inland River: A Case Study of Qingtu Lake in the Shiyang River Basin.* Water, 2019. **11**(8): p. 1673. https://doi.org/10.3390/w11081673
23. Jun, Z., Ming, L., Qiang, C., Min, W., and Xin, P., *Impacts of changing conditions on the ecological environment of the Shiyang River Basin, China.* Water Supply, 2022. **22**(6): p. 5689–5697. https://doi.org/10.2166/ws.2022.197
24. Wang, Q., Shi, J., Chen, G., and Xue, L., *Environmental effects induced by human activities in arid Shiyang River basin, Gansu province, northwest China.* Environ. Geol., 2002. **43**(2002): p. 219-227. https://doi.org/10.1007/s00254-002-0647-3
25. Kang, S., Su, X., Tong, L., Shi, P., Yang, X., and Yukuo, A., *The impacts of human activities on the water–land environment of the Shiyang River basin, an arid region in northwest China.* Hydrol Sci J, 2004. **49** (3): p. 427. https://doi.org/10.1623/hysj.49.3.413.54347
26. Schwilch, G., Bestelmeyer, B., Bunning, S., Critchley, W., Herrick, J., Kellner, K., Liniger, H. P., Nachtergaele, F., Ritsema, C. J., Schuster, B., et al., *Experience in monitoring and assessment of sustainable land management.* Land Degrad. Develop., 2011. **22**: p. 214–225. https://doi.org/10.1002/ldr.1040
27. Vu, Q. M., Le, Q. B., Frossard, E., and Vlek, P. L. G., *Socio-economic and biophysical determinants of land degradation in Vietnam: An integrated causal analysis at the national level.* 2014. **36**: p. 605-617. https://doi.org/10.1016/j.landusepol.2013.10.012
28. Marin, A. M. P., Vendruscolo, J., Salazar, J. R. Z., Queiroz, H. A. A., Magalhães, D. L., Menezes, R. S. C., and Fernandez, I. M., *Monitoring Desertification Using a Small Set of Biophysical Indicators in the Brazilian Semiarid Region.* Sustainability, 2022. **14**(15): p. 9735. https://doi.org/10.3390/su14159735
29. XCerretelli, S., Poggio, L., Gimona, A., Yakob, G., SBoke, S., Habte, M., Coull, M., Peressotti, A., and Black, H., *Spatial assessment of land degradation through key ecosystem services: The role of globally available data.* Sci. Total Environ., 2018. **628-629**: p. 539-555. https://doi.org/10.1016/j.scitotenv.2018.02.085
30. Ramsy, M., Gad, A., Abdelsalam, H., and Siwailam, M., *A dynamic simulation model of desertification in Egypt.* Egypt. J. Remote. Sens. Space Sci., 2010. **13**(2): p. 101-111. https://doi.org/10.1016/j.ejrs.2010.03.001
31. Pulleman, M., Creamer, R., Hamer, U., Helder, J., Pelosi, C., Peres, G., and Rutgers, M., *Soil biodiversity, biological indicators and soil ecosystem services—an overview of European approaches.* COSUST, 2012. **4**(5): p. 529-538. https://doi.org/10.1016/j.cosust.2012.10.009
32. Kader, F. H. A., *Assessment and monitoring of land degradation in the northwest coast region, Egypt using Earth observations data.* Egypt. J. Remote. Sens. Space Sci., 2019. **22**(2). https://doi.org/10.1016/j.ejrs.2018.02.001
33. Rayegani, B., Barati, S., Sohrabi, T. A., and Sonboli, B., *Remotely sensed data capacities to assess soil degradation.* Egypt. J. Remote. Sens. Space Sci., 2016. **19**(2): p. 207-222. https://doi.org/10.1016/j.ejrs.2015.12.001
34. Dubovyk, O., *The role of Remote Sensing in land degradation assessments: opportunities and challenges.* Eur. J. Remote Sens, 2017. **50**(1): p. 601–613. https://doi.org/10.1080/22797254.2017.1378926

35. Lanfredi, M., Coppola, R., Simoniello, T., Coluzzi, R., Emilio, M., Imbrenda, V., and Macchiato, M., *Early Identification of Land Degradation Hotspots in Complex Bio-Geographic Regions.* Remote Sens., 2015. **7**(6): p. 8154-8179. https://doi.org/10.3390/rs70608154
36. Ibrahim, Y., Baltzer, H., Haduk, J., and Tucker, C. J., *Land Degradation Assessment Using Residual Trend Analysis of GIMMS NDVI3g, Soil Moisture and Rainfall in Sub-Saharan West Africa from 1982 to 2012.* Remote Sens., 2015. **7**(5): p. 5471-5494. https://doi.org/10.3390/rs70505471
37. Serrano, S. M. V., Cabello, D., Burguerra, M. T., Hernandez, N. M., Begueria, S., and Molina, C. A., *Drought Variability and Land Degradation in Semiarid Regions: Assessment Using Remote Sensing Data and Drought Indices (1982–2011).* Remote Sens., 2015. **7**(4): p. 4391-4423. https://doi.org/10.3390/rs70404391
38. Lynden, G. W. J. and Mantel, S., *The role of GIS and remote sensing in land degradation assessment and conservation mapping: some user experiences and expectations.* Int J Appl Earth Obs Geoinf, 2001. **3**(1): p. 61-68. https://doi.org/10.1016/S0303-2434(01)85022-4
39. Yu, T., Jiapaer, G., Bao, A., Zheng, G., Jiang, L., Yuan, Y., and Huang, X., *Using Synthetic Remote Sensing Indicators to Monitor the Land Degradation in a Salinized Area.* Remote Sens., 2021. **13**(15): p. 2851. https://doi.org/10.3390/rs13152851
40. Lu, L., Kuenzer, C., Wang, C., Guo, H., and Li, Q., *Evaluation of Three MODIS-Derived Vegetation Index Time Series for Dryland Vegetation Dynamics Monitoring.* Remote Sens., 2015. **7**(6): p. 7597-7614. https://doi.org/10.3390/rs70607597
41. Dubdovik, O., Menz, G., Lee, A., Schellberg, J., Thonfeld, F., and Khamzina, A., *SPOT-Based Sub-Field Level Monitoring of Vegetation Cover Dynamics: A Case of Irrigated Croplands.* Remote Sens., 2015. **7**(6): p. 6763-6783. https://doi.org/10.3390/rs70606763
42. Smith, W. K., Dannenberg, M. P., Yan, D., Hermann, S., Barnes, M. L., Gafford, G. A. B., Biedermn, J. A., Ferrenberg, S., Fox, A. M., and Hudson, A., *Remote sensing of dryland ecosystem structure and function: Progress, challenges, and opportunities.* Remote Sens. Environ., 2019. **233**: p. 111401. https://doi.org/10.1016/j.rse.2019.111401
43. Allen, R. A. W., Ramsey, R. D., West, N. E., and Norton, B. E., *Quantification of the Ecological Resilience of Drylands Using Digital Remote Sensing.* Ecol. Soc., 2008. **13**(1): p. 33.
44. Marzolff, I., Kirchhoff, M., Stephan, R., Seeger, M., Hassaine, A. A., and Ries, J. B., *Monitoring Dryland Trees With Remote Sensing. Part A: Beyond CORONA—Historical HEXAGON Satellite Imagery as a New Data Source for Mapping Open-Canopy Woodlands on the Tree Level.* Front. Environ. Sci., 2022. **10**(896702). https://doi.org/10.3389/fenvs.2022.896702
45. Safaei, M., Bashari, H., Kleinebecker, T., Fakheran, S., Jafari, R., and Stoltenberg, A. G., *Mapping terrestrial ecosystem health in drylands: comparison of field-based information with remotely sensed data at watershed level.* Landsc. Ecol., 2022. https://doi.org/10.1007/s10980-022-01454-4
46. Shang, H., Fan, J., Fan, B., and Su, F., *Economic Effects of Ecological Compensation Policy in Shiyang River Basin: Empirical Research Based on DID and RDD Models.* Sustainability, 2022. **14**(5): p. 2999. https://doi.org/10.3390/su14052999
47. Hu, X., Jin, Y., Ji, L., Zeng, J., Cui, Y., Song, Z., Sun, D., and Cheng, G., *Land use/cover change and its eco-environment effects in Shiyang River Basin*, in *The 4th International Conference on Water Resource and Environment (WRE 2018)*. 2018, IOP Publishing.
48. Wang, Y., Feng, Q., Chen, L., and Yu, T., *Significance and Effect of Ecological Rehabilitation Project in Inland River Basins in Northwest China.* Environ Manage., 2013. **52**: p. 209-220. https://doi.org/10.1007/s00267-013-0077-x
49. Liu, M., Nie Z., Cao, L., Wang, L., Lu, H., Wang, Z., and Zhu, P., *Comprehensive evaluation on the ecological function of groundwater in the Shiyang River watershed.* J. Groundw. Sci. Eng., 2021. **9**(4): p. 326-340. https://doi.org/10.19637/j.cnki.2305-7068.2021.04.006

50. Li, S., Li, X., Gong, J., Dang, D., Dou, H., and Lyu, X., *Quantitative Analysis of Natural and Anthropogenic Factors Influencing Vegetation NDVI Changes in Temperate Drylands from a Spatial Stratified Heterogeneity Perspective: A Case*

Study of Inner Mongolia Grasslands, China. Remote Sens., 2022. **14**(3320). https://doi.org/10.3390/rs14143320

51. Han, X., Jia, G., Yang, G., Wang, N., Liu, F., Chen, H., and Guo, X., *Spatiotemporal dynamic evolution and driving factors of desertification in the Mu Us Sandy Land in 30 years.* Sci Rep, 2020. **10**(21734). https://doi.org/10.1038/s41598-020-78665-9

52. Burrell, A. L., Evans, J. P., and De Kauwe, M. G., *Anthropogenic climate change has driven over 5 million km2 of drylands towards desertification.* Nat.Commun., 2020. **11**(1): p. 3853. https://doi.org/10.1038/s41467-020-17710-7

53. Fan, Z., Li, S., and Fang, H., *Explicitly Identifying the Desertification Change in CMREC Area Based on Multisource Remote Data.* Remote Sens., 2020. **12**(19): p. 3170. https://doi.org/10.3390/rs12193170

54. Hien, L. T. T., Gobin, A., and Huong, P. T. T., *Spatial indicators for desertification in southeast Vietnam.* Earth Syst. Sci., 2019. **19**: p. 2325–2337. https://doi.org/10.5194/nhess-19-2325-2019, 2019

55. Guo, Q., Fu, B., Shi, P., Thomas, C., Zhang, J., and Xu, H., *Satellite Monitoring the Spatial-Temporal Dynamics of Desertification in Response to Climate Change and Human Activities across the Ordos Plateau, China.* Remote Sens., 2017. **9**(6): p. 525. https://doi.org/10.3390/rs9060525

56. Zhang, J., Guan, Q., Du, Q., Ni, F., Mi, J., Luo, H., and Shao, W., *Spatial and temporal dynamics of desertification and its driving mechanism in Hexi region.* Land Degrad Dev, 2022. **33**(17): p. 3539-3556. https://doi.org/10.1002/ldr.4407

57. Zhou, W., Sun, Z., Li, J., Gang, C., and Zhang, C., *Desertification dynamic and the relative roles of climate change and human activities in desertification in the Heihe River Basin based on NPP.* J. Arid Land, 2013. **5,**: p. 465–479 https://doi.org/10.1007/s40333-013-0181-z

58. Meng, X., Gao, X., Li, S., Li, S., and Lei, J., *Monitoring desertification in Mongolia based on Landsat images and Google Earth Engine from 1990 to 2020.* Ecol. Indic., 2021. **129**: p. 107908. https://doi.org/10.1016/j.ecolind.2021.107908

59. Wang, J. and Xu, C., *Geodetector: Principle and prospective.* Acta Geogr. Sin., 2017. **72**(1): p. 116-134. https://doi.org/10.11821/dlxb201701010

60. Zhang, S., Zhou, Y., Yu, Y., Li, F., Zhang, R., and Li, W., *Using the Geodetector Method to Characterize the*

Spatiotemporal Dynamics of Vegetation and Its Interaction with Environmental Factors in the Qinba Mountains, China. Remote Sens., 2022. **14**: p. 5794. https://doi.org/10.3390/rs14225794

61. Ren, D. and Caio, A., *Analysis of the heterogeneity of landscape risk evolution and driving factors based on a combined GeoDa and Geodetector model.* Ecol. Indic., 2022. **144**: p. 109568. https://doi.org/10.1016/j.ecolind.2022.109568

62. Wang, B. and Gao, X., *Temporal and spatial variations of water resources constraint intensity on urbanization in the Shiyang River Basin, China.* Environ Dev Sustain, 2021. **23**: p. 10038–10055. https://doi.org/10.1007/s10668-020-01045-w

63. Zhu, G., Wan, Q., TYong, L., Zhang, Z., Guo, H., Zhang, Y., Sun, Z., Zhang, Z., and Ma, H., *Dissolved organic carbon transport in the Qilian mountainous areas of China.* Hydrol. Process., 2020. **34**: p. 4985–4995. https://doi.org/10.1002/hyp.13918

64. Hu, L., Wang, Z., Tian, W., and Zhao, J., *Coupled surface water-groundwater model and its application in the arid Shiyang River basin, China.* Hydrol. Process. Int. J., 2009. **23**: p. 2033–2044. https://doi.org/10.1002/hyp.7333

65. Wang, Z., Shi, P., Zhang, X., Tong, H., Zhang, W., and Liu, Y., *Research on Landscape Pattern Construction and Ecological Restoration of Jiuquan City Based on Ecological Security Evaluation.* sustainability, 2021. **13**(10). https://doi.org/10.3390/su13105732

66. Wang, H., Zhang, M., Zhu, H., Dang, X., Ynang, Z., and Yin, L., *Hydro-climatic trends in the last 50 years in the lower reach of the Shiyang RiverBasin, NW China.* catena, 2012. **95**: p. 33-41.
67. Su, X., Singh, V. P., Niu, J., and Hao, L., *Spatiotemporal trends of aridity index in Shiyang River basin of northwest China.* Stoch Environ Res Risk Assess 2015. **29**(6): p. 1571-1582. https://doi.org/10.1007/s00477-015-1082-9
68. Wang, Z., Ficklin, D. L., Zhang, Y., and Zhang, M., *Impact of climate change on streamflow in the arid Shiyang River Basin of northwest China.* Hydrol. Process., 2011. **26**(18): p. 2733-2744. https://doi.org/10.1002/hyp.8378
69. Zhang, Y., Jiang, J., Shen, B., Shen, Q., Yang, D., Tian, F., Tang, L., and Liu, Z. *Study on countermeasures for water resources shortage and changes of ecological environment in Shiyang River basin*. 2008.
70. Bao, C. and Fang, C., *Water resources constraint force on urbanization in water deficient regions: A case study of the Hexi Corridor, arid area of NW China.* Ecol Econ, 2007. **62**: p. 508 – 517. https://doi.org/10.1016/j.ecolecon.2006.07.013
71. Chen, M., Wang, P., and Chen, L., *Population Distribution Evolution Characteristics and Shift Growth Analysis in Shiyang River Basin.* J.Geosci, 2014. **5**(11): p. 1395-1403. https://doi.org/10.4236/ijg.2014.511113
72. Deng, X., Wilson, J. P., and Gallant, J. C., *Terrain Analysis*, in *The Handbook of Geographic Information Science*, J.P. Wilson and A.S. Fotheringham, Editors. 2007.
73. Guan, Q., Yang., L., Pan, N., Lin, J., Xu, C., Wang, F., and Liu, Z., *Greening and Browning of the Hexi Corridor in Northwest China: Spatial Patterns and Responses to Climatic Variability and Anthropogenic Drivers.* Remote Sens., 2018. **10**: p. 1270. https://doi.org/10.3390/rs10081270
74. Jiang, Y., Du, W., Chen, J., Wang, C., Wang, J., Sun, W., Chai, X., Ma, L., and Xu, Z., *Climatic and Topographical Effects on the Spatiotemporal Variations of Vegetation in Hexi Corridor, Northwestern China.* Diversity 2022. **14**: p. 370. https://doi.org/. https://doi.org/10.3390/d14050370
75. Safanelli, J. L., Poppiel, R. R., Ruiz, L. F. C., Bonfatti, B. R., Mello, F. A. M., Rizzo, R., and Demattê, J. A. M., *Terrain Analysis in Google Earth Engine: A Method Adapted for High-Performance Global-Scale Analysis.* ISPRS Int. J. Geo-Inf., 2020. **9**: p. 400. https://doi.org/10.3390/ijgi9060400
76. Zhang, L., Wu, B., Xi, X., and Xing, Q., *Classification system of China land cover for carbon budget.* Acta Ecol. Sin, 2014. **34**(24): p. 7158-7166. https://doi.org/10.5846/stxb201310102431
77. Stavi, I., Thevs, N., and Priori, S., *Soil Salinity and Sodicity in Drylands: A Review of Causes, Effects, Monitoring, and Restoration Measures.* Front. environ. sci, 2021. **9**(712831). https://doi.org/10.3389/fenvs.2021.712831
78. Hassani, A., Azapagic, A., and Shokri, N., *Global predictions of primary soil salinization under changing climate in the 21st century.* Nat Commun, 2021. **12**(6663). https://doi.org/10.1038/s41467-021-26907-3
79. Ngabire, M., Wang, T., Xue, X., Liao, J., Ghada, S., Huang, C., Duan, H., and Song, X., *Soil salinization mapping across different sandy land-cover types in the Shiyang River Basin: A remote sensing and multiple linear regression approach.* RSASE, 2022. **28**: p. 100847. https://doi.org/10.1016/j.rsase.2022.100847
80. Zhang, X. and Zhao, Y., *Identification of the driving factors' influences on regional energy-related carbon emissions in China based on geographical detector method.* Environ Sci Pollut Res, 2018. **25**: p. 9626–9635. https://doi.org/10.1007/s11356-018-1237-6
81. Escobedo, F. J. and Nowak, D. J., *Spatial heterogeneity and air pollution removal by an urban forest.* Landsc Urban Plan, 2009. **90**(3-4): p. 102-110. https://doi.org/10.1016/j.landurbplan.2008.10.021
82. Xu, Y., Li, P., Pan, J., Zhang, Y., Dang, X., Cao, X., Cui, J., and Yang, Z., *Eco-Environmental Effects and Spatial Heterogeneity of "Production-Ecology-Living" Land Use Transformation: A Case Study for Ningxia, China.* Sustainability, 2022. **14**(15): p. 9659. https://doi.org/10.3390/su14159659
83. Yin, H., Chen, C., Dong, Q., Zhang, P., Chen, Q., and Zhu, L., *Analysis of Spatial Heterogeneity and Influencing Factors of Ecological Environment Quality in China's North-South Transitional Zone.* Int. J. Environ. Res. Public Health 2022. **19**(5): p. 2236. https://doi.org/10.3390/ijerph19042236

84. Wang, H., Qin, F., Xu, C., Li, B., Guo, L., and Wang, Z., *Evaluating the suitability of urban development land with a Geodetector.* Ecol. Indic., 2021. **123**: p. 107339. https://doi.org/10.1016/j.ecolind.2021.107339

85. Liang, X., Li, P., Wang, J., Chan, F. K., Togtokh, C., Ochir, A., and Davaasuren, D., *Research Progress of Desertification and Its Prevention in*

Mongolia. Sustainability, 2021. **13**: p. 6861. https://doi.org/10.3390/su13126861

86. Zhang, Z., Song, Y., and Wu, P., *Robust geographical detector.* Int J Appl Earth Obs Geoinf 2022. **109**(102782). https://doi.org/10.1016/j.jag.2022.102782

87. Song, Y., Wang, J., Ge, Y., and Xu, C., *An optimal parameters-based geographical detector model enhances geographic characteristics of explanatory variables for spatial heterogeneity analysis: cases with different types of spatial data.* GIsci Remote Sens, 2020. **57**(5): p. 593-610. https://doi.org/10.1080/15481603.2020.1760434

88. Wang, F., Li, X., Christakos, G., Liao, Y., Zhang, T., and Gu, X., *Geographical Detectors-Based Health Risk Assessment and its Application in the Neural Tube Defects Study of the Heshun Region, China.* Int J Geogr Inf Sci, 2010. **24**(1): p. 107-127. https://doi.org/10.1080/13658810802443457

89. Wang, T. and Watson, J., *Scenario analysis of China's emissions pathways in the 21st century for low carbon transition.* Energy Policy, 2010. **38**(7): p. 3537-3546. https://doi.org/10.1016/j.enpol.2010.02.031

90. Ding, Y., Zhang, M., Qian, X., Li, C., Chen, S., and Wang, W., *Using the geographical detector technique to explore the impact of socioeconomic factors on PM2.5 concentrations in China.* J. Clean. Prod., 2019. **211**: p. 1480-1490. https://doi.org/10.1016/j.jclepro.2018.11.159

91. Cao, F., Ge, Y., and Wang, J., *Optimal discretization for geographical detectors-based risk assessment.* GIsci Remote Sens, 2013. **50**(1). https://doi.org/10.1080/15481603.2013.778562

92. Wu, R., Zhang, J., Bao, Y., and Zhang, F., *Geographical Detector Model for Influencing Factors of Industrial Sector Carbon Dioxide Emissions in Inner Mongolia, China.* Sustainability, 2016. **8**(2): p. 149. https://doi.org/10.3390/su8020149

93. Jia, W., Wang, M., Zhou, C., and Yang, Q., *Analysis of the spatial association of geographical detector-based landslides and environmental factors in the southeastern Tibetan Plateau, China.* PLoS One, 2021. **16**(5): p. e0251776. https://doi.org/10.1371/journal.pone.0251776

94. Wang, J. and Hu, Y., *Environmental health risk detection with GeogDetector*. Environ Model Softw, 2012. **33**: p. 114–115. https://doi.org/10.1016/j.envsoft.2012.01.015

95. Han, J., Wang, J., Chen, L., Xiang, J., Ling, Z., Li, Q., and Wang, E., *Driving factors of desertification in Qaidam Basin, China: An 18-year analysis using the geographic detector model.* Ecol. Indic., 2021. **124**: p. 107404. https://doi.org/10.1016/j.ecolind.2021.107404

96. Alvarez, L. J., Epstein, H. E., Li, J., and Okin, G. S., *Aeolian process effects on vegetation communities in an arid grassland ecosystem.* Ecol Evol, 2012. **2**(4): p. 809–821. https://doi.org/10.1002/ece3.205

97. Glenn, E. P., Huete, A. R., Nagler, P. L., and Nelson, S. G., *Relationship Between Remotely-sensed Vegetation Indices, Canopy Attributes and Plant Physiological Processes: What Vegetation Indices Can and Cannot Tell Us About the Landscape.* Sensors, 2008. **8**(4): p. 2136-2160. https://doi.org/10.3390/s8042136

98. Gao, L., Wang, X., Johnson, B. A., Tian, Q., Wang, Y., Verrelst, J., Mu, X., and Gu, X., *Remote sensing algorithms for estimation of fractional vegetation cover using pure vegetation index values: A review.* ISPRS Int. J. Geo-Inf, 2020. **159**: p. 364-377. https://doi.org/10.1016/j.isprsjprs.2019.11.018

99. Choi, S. K., Jung, S. H., and Choi, D. Y., *Estimation of Fractional Vegetation Cover in Sand Dunes Using Multi-spectral Images from Fixed-wing UAV.* J. Korean Soc. Surv. Geod. Photogramm. Cartogr., 2016. **34**(4): p. 431-441. https://doi.org/10.7848/ksgpc.2016.34.4.431

100. Ding, Y., Zhang, H., Li, Z., Xin, X., Zheng, X., and Zhao, K., *Comparison of fractional vegetation cover estimations using dimidiate pixel models and look-up table inversions of the PROSAIL model from Landsat 8 OLI data.* J. Appl. Remote Sens., 2016. **10**(3): p. 036022. https://doi.org/10.1117/1.JRS.10.036022

101. Zeng, X., Doickson, R. E., Alison, W., Muhammad, S., Ruth, D. S., and Qi, J., *Derivation and Evaluation of Global 1-km Fractional Vegetation Cover Data for Land Modeling.* J. Appl. Meteorol., 2000. **39**(6): p. 826-839. https://doi.org/10.1175/1520-0450(2000)039<0826:DAEOGK>2.0.CO;2

102. Liu, Y., Li, Y., Cui, C., and Ruan, H., *Evaluation of MODIS MOD13Q1 data in desertification in the north area of Xinjiang.* Acta Prataculturae Sin., 2010. **19**: p. 14-21.

103. Reynolds, J. F., Maestre, F. T., Kemp, P. R., Smith, D. M. S., and Lambin, E., *Natural and Human Dimensions of Land Degradation in Drylands: Causes and Consequences*, in *Terrestrial Ecosystems in a Changing World. Global Change*, J.G. Canadell, D.E. Pataki, and L.F. Pitelka, Editors. 2007. p. 247-257.

104. Ngabire, M., Wang, T., Xue, X., Liao, J., Sahbeni, G., Huang, C., Xiang, S., and Duan, H., *Synergic effects of land-use management systems towards the reclamation of Aeolian Desertified Land in the Shiyang River Basin.* Ecol. Indic., 2022. **139**(2022): p. 108882. https://doi.org/10.1016/j.ecolind.2022.108882

105. Liao, J., Wang, T., and Ma, S., *Mapping the dynamic degree of aeolian desertification in the Shiyang River Basin from 1975 to 2010.* Sci. Cold Arid. Reg, 2020. **12**(3). https://doi.org/10.3724/SP.J.1226.2020.00144

106. Shao, Y., Dong, Z., Meng, J., Wu, S., Zhu, S., Zhang, Q., and Zheng, Z., *Analysis of Runoff Variation and Future Trends in a Changing Environment: Case Study for Shiyanghe River Basin, Northwest China.* sustainability, 2023. **15**: p. 2173. https://doi.org/10.3390/su15032173

107. Xu, C. D., Wang, R. R., Ding, L. Y., and Wen, Q. Y., *Study on the Climate Change of Shiyang River Basin in Chinese Arid Inland Area.* CEt, 2015. **46**(2015). https://doi.org/10.3303/CET1546129

108. Zhang, C. and Li, Y., *Verification of watershed vegetation restoration policies, arid China.* Sci Rep, 2016. **6**(30740). https://doi.org/10.1038/srep30740

109. Zhu, Q. and Li, Y., *Environmental Restoration in the Shiyang River Basin, China: Conservation, Reallocation and More Efficient Use of Water.* Aquat. Procedia, 2014. **2**(2014): p. 24-34. https://doi.org/10.1016/j.aqpro.2014.07.005

110. Tang, Z., Ma, J., Peng, H., Wang, S., and Wei, J., *Spatiotemporal changes of vegetation and their responsesto temperature and precipitation in upper Shiyang river basin.* Adv. Space Res., 2017. **60** (5): p. 969-979. https://doi.org/10.1016/j.asr.2017.05.033

111. Ma, Q., Wang, X., Chen, F., Wei, L., Zhang, D., and Jin, H., *Carbon sequestration of sand-fixing plantation of Haloxylon ammodendron in Shiyang River Basin: Storage, rate and potential.* Glob. Ecol, 2021. **28**(2021). https://doi.org/10.1016/j.gecco.2021.e01607

112. Lancaster, N., *Response of Aeolian Processes and Landforms to Climate Change and Variability*, in *Treatise on Geomorphology (Second Edition)*. 2022. p. 318-339.

113. Zhang, F., Wang, C., and Wang, Z., *Response of Natural Vegetation to Climate in Dryland Ecosystems: A Comparative Study between Xinjiang and Arizona.* Remote Sens., 2020. **12**(21): p. 3567. https://doi.org/10.3390/rs12213567

114. Mayaud, J. R. and Webb, N. P., *Vegetation in Drylands: Effects on Wind Flow and Aeolian Sediment Transport.* land, 2017. **6**(3): p. 64. https://doi.org/10.3390/land6030064

115. Lancaster, N., *Response of eolian geomorphic systems to minor climate change: examples from the southern Californian deserts.* Geomorphology, 1997. **19**(3-4): p. 333-347. https://doi.org/10.1016/S0169-555X(97)00018-4

116. Heindel, R. C., Culler, L. E., and Virginia, R. A., *Rates and processes of aeolian soil erosion in West Greenland.* The Holocene, 2017. **27**(9). https://doi.org/10.1177/0959683616687381

117. Catto, N. R. and Bachhuber, F. W., *Aeolian Geomorphic Response to Climate Change: An Example from the Estancia Valley, Central New Mexico, USA*, in *Linking Climate Change to Land Surface Change*, S.J. McLaren and D.R. Kniveton, Editors. 2000, Springer: Dordrecht.

118. Dousari, A. A., Ramadan, A., Qattan, A. A., Arteeqi, S. A., Dashti, H., Ahmed, M., Dousari, N. A., Hashash, N. A., and Othman, A., *Cost and effect of native vegetation change on aeolian sand, dust, microclimate and sustainable energy in Kuwait.* J. Taibah Univ. Sci., 2020. **14**(1): p. 628-639. https://doi.org/10.1080/16583655.2020.1761662

119. Edwards, B. L., Webb, N. P., Brown, D. P., Elias, E., Peck, D. E., Pierson, F. B., Williams, C. J., and Herrick, J. E., *Climate change impacts on wind and water erosion on US rangelands.* J Soil Water Conserv, 2019. **74**(4). https://doi.org/10.2489/jswc.74.4.405

120. Zhao, C., Li, X., Zhou, X., Zhao, K., and yang, Q., *Holocene Vegetation Succession and Response to Climate Change on the South Bank of the Heilongjiang-Amur River, Mohe County, Northeast China.* Adv. Meteorol., 2016. **2450697**: p. 1-11. https://doi.org/10.1155/2016/2450697

121. Singh, G., Tomar, U. K., Singh, B., and Sharma, S., *A Manual for Dryland Afforestation and Management*. 2017: Scientific Publishers - AFARI.

122. Wu, J., Kurosaki, Y., and Du, C., *Evaluation of Climatic and Anthropogenic Impacts on Dust Erodibility: A Case Study in Xilingol Grassland, China.* Sustainability, 2020. **12**(629). https://doi.org/10.3390/su12020629

123. Ishizuka, M., Mikami, M., and Yamada, Y., Zeng,F.,, *Threshold Friction Velocities of Saltation Sand Particles for Different Soil Moisture Conditions in the Taklimakan Desert.* SOLA, 2009. **5**: p. 184–187. https://doi.org/10.2151/sola.2009–047

124. Dregne, H. E., *Physics of desertification* in *Desertification of Arid Lands*, F. El-Baz and M.H.A. Hassan, Editors. 1986, Springer: Dordrecht.

125. Lin, N. F. and Tang, J., *Geological environment and causes for desertification in arid-semiarid regions in China.* Env Geol, 2002. **41**: p. 806–815. https://doi.org/10.1007/s00254-001-0456-0

126. Chen, N., Guo, C., Li, Z., and Liu, L., *The grassland degradation problems of the Minqin oasis, in the lower reaches of the Shiyang River Basin.* Acta Prataculturae Sinica, 2010. **19**(6): p. 62-71.

127. Li, B., *Soil Salinization*, in *Desertification and Its Control in China*. 2010, Springer: Berlin, Heidelberg.

128. Wang, Y. and Qin, D., *Influence of climate change and human activity on water resources in arid region of Northwest China: An overview.* Adv. Clim. Chang. Res., 2017. **8**(4): p. 268-278. https://doi.org/10.1016/j.accre.2017.08.004

129. Yang, J., Zhao, J., Zhu, G., Wang, Y., Ma, X., Wang, J., Guo, H., and Zhang, Y., *Soil salinization in the oasis areas of downstream inland rivers —Case Study: Minqin oasis.* Math. Probl. Eng., 2020. **537**: p. 69-78. https://doi.org/10.1016/j.quaint.2020.01.001

130. Li, F., Zhu, G., and Guo, C., *Shiyang River ecosystem problems and countermeasures* Int. J. Agric. Sci., 2013. **4**(2): p. 72-78 https://doi.org/10.4236/as.2013.42012.

131. Castellini, M., Di Prima, S., Stewart, R., Biddocu, M., Rahmati, M., and Alagna, V., *Advances in Ecohydrology for Water Resources Optimization in Arid and Semi-Arid Areas.* Water, 2022. **14**(1830). https://doi.org/10.3390/w14121830

132. Wei, W., Shi, P., Zhao, J., Wang, X., and Wang, X., *Environmental Suitability Evaluation for Human Settlements in Arid Inland River Basin-A Case Study on the Shiyang River Basin.* Adv Mat Res, 2012. **518-523**: p. 4874-4884. https://doi.org/10.4028/www.scientific.net/AMR.518-523

133. Kang, S., Su, X., Tong, L., Zhang, J., and Zhang, L., *A warning from an ancient oasis: intensive human activities are leading to potential ecological and social catastrophe.* Int. J. Sustain. Dev, 2010. **15**(5): p. 440-447. https://doi.org/10.3843/SusDev.15.5:5

134. Jun, Z., Ming, L., Qiang, C., Min, W., and Xin, P., *Impacts of changing conditions on the ecological environment of the Shiyang River Basin, China.* Water Supply, 2022. **22**(6): p. 5689. https://doi.org/10.2166/ws.2022.197

135. Du, Z., Xu, X., Zhang, H., Wu, Z., and Liu, Y., *Geographical Detector-Based Identification of the Impact of Major Determinants on Aeolian Desertification Risk.* PLoS One, 2016. **11**(3): p. e0151331. https://doi.org/10.1371/journal.pone.0151331

136. Xu, C., Li, Y., Wang, J., and Xiao, G., *Spatial-temporal detection of risk factors for bacillary dysentery in Beijing, Tianjin and Hebei, China.* BMC Public Health., 2017. **17**: p. 743. https://doi.org/10.1186/s12889-017-4762-1

137. Yue, H. and Hu, T., *Geographical Detector-Based Spatial Modeling of the COVID-19 Mortality Rate in the Continental United States.* Int J Environ Res Public Health, 2021. **18**(13): p. 6832. https://doi.org/10.3390/ijerph18136832